


RESEARCH ARTICLE

Open Access



Re-annotation of the *Theileria parva* genome refines 53% of the proteome and uncovers essential components of N-glycosylation, a conserved pathway in many organisms

Kyle Tretina¹, Roger Pelle², Joshua Orvis¹, Hanzel T. Gotia¹, Olukemi O. Ifeonu¹, Priti Kumari¹, Nicholas C. Palmateer¹, Shaikh B. A. Iqbal¹, Lindsay M. Fry^{3,4}, Vishvanath M. Nene⁵, Claudia A. Daubenberger^{6,7}, Richard P. Bishop⁴ and Joana C. Silva^{1,8*} 

Abstract

Background: The apicomplexan parasite *Theileria parva* causes a livestock disease called East coast fever (ECF), with millions of animals at risk in sub-Saharan East and Southern Africa, the geographic distribution of *T. parva*. Over a million bovines die each year of ECF, with a tremendous economic burden to pastoralists in endemic countries. Comprehensive, accurate parasite genome annotation can facilitate the discovery of novel chemotherapeutic targets for disease treatment, as well as elucidate the biology of the parasite. However, genome annotation remains a significant challenge because of limitations in the quality and quantity of the data being used to inform the location and function of protein-coding genes and, when RNA data are used, the underlying biological complexity of the processes involved in gene expression. Here, we apply our recently published RNAseq dataset derived from the schizont life-cycle stage of *T. parva* to update structural and functional gene annotations across the entire nuclear genome.

Results: The re-annotation effort led to evidence-supported updates in over half of all protein-coding sequence (CDS) predictions, including exon changes, gene merges and gene splitting, an increase in average CDS length of approximately 50 base pairs, and the identification of 128 new genes. Among the new genes identified were those involved in N-glycosylation, a process previously thought not to exist in this organism and a potentially new chemotherapeutic target pathway for treating ECF. Alternatively-spliced genes were identified, and antisense and multi-gene family transcription were extensively characterized.

(Continued on next page)

* Correspondence: jcsilva@som.umaryland.edu

¹Institute for Genome Sciences, University of Maryland School of Medicine, Baltimore, MD 21201, USA

⁸Department of Microbiology and Immunology, University of Maryland School of Medicine, Baltimore, MD 21201, USA

Full list of author information is available at the end of the article



© The Author(s). 2020 **Open Access** This article is licensed under a Creative Commons Attribution 4.0 International License, which permits use, sharing, adaptation, distribution and reproduction in any medium or format, as long as you give appropriate credit to the original author(s) and the source, provide a link to the Creative Commons licence, and indicate if changes were made. The images or other third party material in this article are included in the article's Creative Commons licence, unless indicated otherwise in a credit line to the material. If material is not included in the article's Creative Commons licence and your intended use is not permitted by statutory regulation or exceeds the permitted use, you will need to obtain permission directly from the copyright holder. To view a copy of this licence, visit <http://creativecommons.org/licenses/by/4.0/>. The Creative Commons Public Domain Dedication waiver (<http://creativecommons.org/publicdomain/zero/1.0/>) applies to the data made available in this article, unless otherwise stated in a credit line to the data.

(Continued from previous page)

Conclusions: The process of re-annotation led to novel insights into the organization and expression profiles of protein-coding sequences in this parasite, and uncovered a minimal N-glycosylation pathway that changes our current understanding of the evolution of this post-translational modification in apicomplexan parasites.

Keywords: *Theileria*, East coast fever, Genome, Re-annotation, N-glycosylation

Background

East Coast fever (ECF) in eastern, central, and southern Africa causes an estimated loss of over 1 million heads of cattle yearly, with an annual economic loss that surpasses \$300 million USD, impacting mainly smallholder farmers [1]. Cattle are the most valuable possession of smallholder farmers in this region, as they are a source of milk, meat and hides, provide manure and traction in mixed crop-livestock systems, and revenue derived from livestock pays for school fees and dowries [2, 3]. ECF is a tick-transmitted disease caused by the apicomplexan parasite *Theileria parva*. Lymphocytes infected with *T. parva* proliferate in the regional lymph node draining the tick bite site, and then metastasize into various lymphoid and non-lymphoid organs, and induce a severe inflammatory reaction that leads to respiratory failure and death of susceptible cattle, which typically die within three to four weeks of infection [4–7]. *T. parva* control is vital to food security in this region of the world, which is plagued by a range of other infectious diseases of humans and their livestock.

Efficacious and affordable chemotherapeutics and vaccines are essential tools in the effective control of infectious disease agents [8, 9]. A reliable structural annotation of the genome, consisting at minimum of the correct location of all protein-coding sequences (CDSs), enables the identification, prioritization and experimental screening of potential vaccine and drug targets [10–12]. The accurate identification of the complete proteome can greatly enhance microbiological studies, and reveals metabolic processes unique to pathogens [13]. In turn, a better understanding of the biology of *T. parva* transmission, colonization and pathogenesis may ultimately reveal novel targets for pathogen control [14]. Currently, much like for other apicomplexan parasites [15, 16], knowledge on the functional role of genomic sequences outside of *T. parva* CDSs is sparse, and many gene models containing only CDSs are supported by little or no experimental evidence. RNAseq data, generated through deep sequencing of cDNA using next generation sequencing technologies, can provide an extraordinary level of insight into gene structure and regulation [12, 17]. Here, we used the first high-coverage RNAseq data for this species [18] to improve existing gene models through the identification of start and stop codons, primary intron splice sites and untranslated regions (UTRs). While RNAseq data exists in publicly available databases for other, closely related

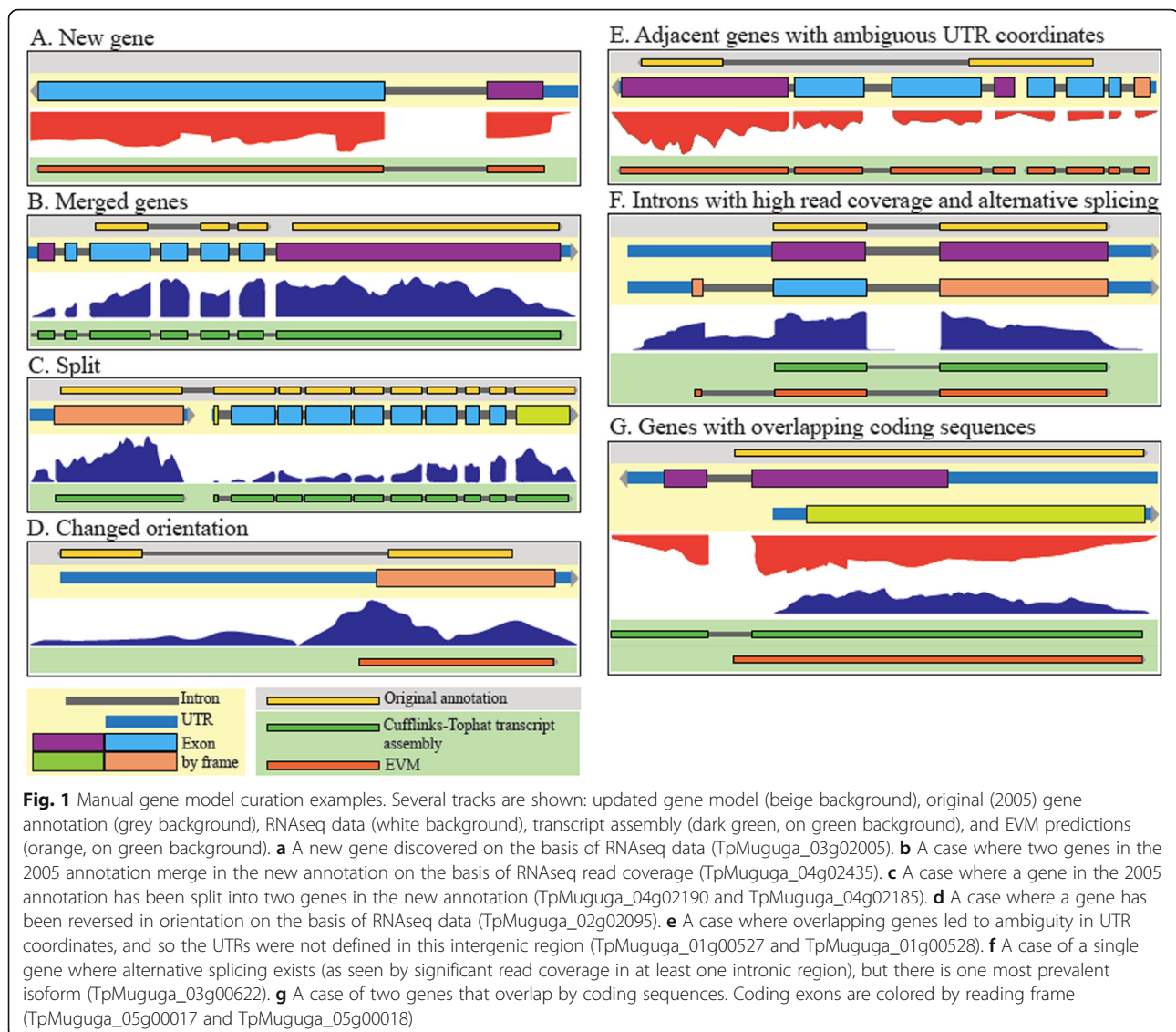
pathogens, such as *Theileria annulata* and *Babesia bovis*, recent systematic re-annotation efforts for these genomes have yet to be published. This new gene model annotation brought to light several new insights into gene expression in this gene-dense eukaryote, and led to the discovery of several new prospective chemotherapeutic targets for treating ECF.

Results

The annotation of the *Theileria parva* genome is significantly improved, revealing a higher gene density than previously thought

The nuclear genome of the reference *T. parva* Muguga isolate consists of four linear chromosomes which are currently assembled into eight contigs (Supplementary Table S1, Additional File 1): chromosomes 1 and 2 are assembled into a single contig each, chromosome 3 is in four contigs and chromosome 4 in two [19]. The new genome annotation was based on this assembly and on extensive RNAseq data (Supplementary Figure S1, Additional File 1). We performed a comprehensive revision of the entire *T. parva* genome annotation, including automated structural annotation and a double-pass manual curation of each locus (see Methods).

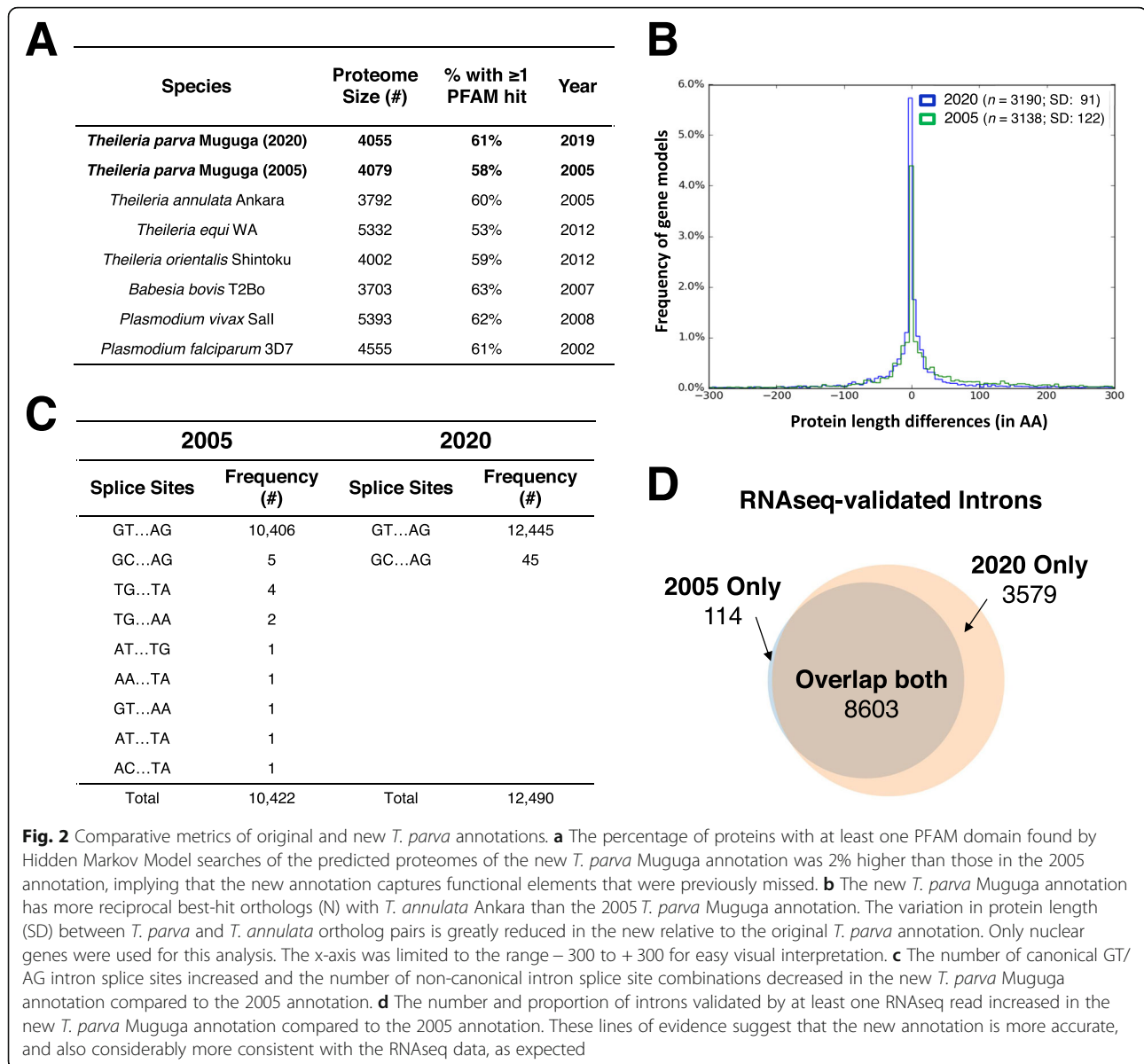
The re-annotation process resulted in the discovery of 128 new genes, 274 adjacent gene models were merged, 157 gene models were split, and 38 genes were replaced by new genes encoded in the reverse orientation (Fig. 1). In addition, exon boundaries have been corrected in over a thousand genes. Overall, 83% of all nuclear genes in the original annotation were altered in some way, with changes made on every contig. This resulted in significant alterations to the predicted proteome, with 53% of the nuclear proteins in the original annotation having altered amino acid sequences in the new annotation, a remarkable ~ 50 bp increase in average CDS length, a reduction of the average length of intergenic regions by close to 100 bp and the assignment of an additional 200,000 base pairs (or 2.4% of the genome), previously classified as intergenic or intronic sequences, to the proteome. This results in a genome that is denser than previously thought, with an overall increase in the coding fraction of the genome from 68 to 71%, more closely resembling *T. annulata* Ankara, which has a coding fraction of 72.9% (Supplementary Table S2, Additional File 1). In fact, *T. parva* has the densest genome out of the indicated genomes investigated,



with one protein-coding gene every ~ 2100 bp (Supplementary Table S2, Additional File 1).

Several lines of evidence suggest that this annotation represents a very significant improvement of the *T. parva* proteome relative to the original annotation. First, there was an increase in the proportion of proteins with at least one PFAM domain in the new proteome compared to the original proteome, implying that the new annotation captures functional elements that were previously missed (Fig. 2a). Given the close evolutionary relationship and near complete synteny between *T. parva* and *T. annulata* [20], their respective proteomes are expected to be very similar. Indeed, a comparison of the two predicted proteomes results in 52 additional reciprocal best hits and protein length differences between orthologs in *T. parva* and *T. annulata* also decreased significantly (Fig. 2b). It is likely that some of the most significant differences

between the *T. parva* and *T. annulata* proteomes, in particular the 25% fewer protein-coding genes and much longer CDSs in the latter, represent annotation errors in the *T. annulata* genome that will be corrected upon revision with more recently accumulated evidence. The total number of non-canonical splice sites in the genome increased from 0.15 to 0.36% of all introns, but the sequence diversity of non-canonical splice sites decreased from eight non-canonical splice donor and acceptor site combinations to only a single splice site pair – GC/AG donor and acceptor dinucleotides, recognized by the U2-type spliceosome [21] (Fig. 2c). The new annotation is also considerably more consistent with the RNAseq data, with a larger number of introns, a higher proportion of which is supported by at least one RNAseq read (Fig. 2d). A total of 118 introns from the original genome annotation have been removed, due to contradicting RNAseq evidence.



The tremendous power of RNAseq to inform on gene and isoform structure in this species revealed a significant amount of transcriptome diversity and complexity. First, the proportion of loci (defined here as a continuous genomic region encoding the length of a CDS, intervening introns, and flanking UTRs) that appear to overlap an adjacent locus increased from 2 to 29% in the new annotation. In many of these instances, read coverage, coding potential, and other evidence support the presence of adjacent genes with overlapping UTRs (Supplemental Figure S2a). In 130 cases, the overlap includes not only UTRs but also CDSs (Supplemental Figure S2b). Secondly, there are many instances of overlapping loci in which the respective CDSs are encoded in the same strand; in these cases, no UTRs were defined in the intervening intergenic region, since

their exact boundaries could not be determined (Additional File 2). Finally, during manual curation, we observed many instances of potential alternative splicing, the clearest of which were the cases of well-supported introns where RNAseq coverage was nevertheless significantly higher than zero (Supplemental Figure S3; Fig. 1f). In fact, we identified 872 introns, in 490 expressed genes (with average read coverage > 0), where the read coverage was at least equal to the mean read coverage for the coding sequences of the respective gene (Supplemental Figure S3b,c; Additional File 3), instances that are only possible to detect when read coverage varies considerably across the gene, which is not uncommon (e.g. Fig. 1c,e). In these cases, only the most prevalent isoform was annotated (Fig. 1f). Finally, despite its power, RNAseq evidence is not sufficient to resolve the

structure of all loci; when the evidence did not clearly favor one gene model over another, the gene model in the original annotation was maintained by default. Interestingly, the vast majority of the genes appear to have only one or, sometimes, two most prevalent isoforms, as has been proposed for *Plasmodium* [22], although this was not defined quantitatively here. The median length of the annotated mRNA reported here is ~1500 bp, and the maximum length > 15,000 bp (Supplementary Figure S4, Additional File 1).

Most genes are transcribed during the schizont stage of the *Theileria parva* life-cycle, and antisense transcription is widespread

We sequenced cDNA generated from polyA-enriched total RNA collected from a *T. parva*-infected, schizont-transformed bovine cell line (see Methods section). A total of 8.3×10^7 paired-end reads were obtained with an Illumina HiSeq 2000 platform, 70.04% of which mapped to the *T. parva* reference genome (Supplementary Table S1, Additional File 1). RNAseq provided a complete and quantitative view of transcription revealing that most of the genome of this parasite is transcribed during the schizont stage of its life cycle (Supplementary Figures S3, S5, Additional File 1). We found that 4011 of all 4054 (98%) predicted protein-coding parasite genes are transcribed at the schizont stage, and 12,172 of all 12,296 introns are supported by RNAseq reads (Fig. 2d). We found evidence of expression for almost all of the known humoral and cellular immunity antigens (Supplementary Table S3, Additional File 1). In fact, Tp9, one of those antigens, is among the 15 most highly expressed genes in our dataset (Supplementary Table S4, Additional File 1). Interestingly, its ortholog in *T. annulata* has been hypothesized to contribute to schizont-induced host cell transformation [23].

As has recently been suggested from in silico analyses [18], transcription in *T. parva* occurs from diverse kinds of promoters, with many instances of adjacent loci overlapping on the same or opposite strands. In fact, of the 4085 predicted protein-coding nuclear genes, only 74 had an estimated reads per kilobase of transcript per million reads (RPKM) of zero and an additional 154 had RPKM < 1. Interestingly, of the 74 genes with an RPKM of zero, most are hypothetical, with no predicted functional annotation, and without any high-confidence orthologs (Supplementary Table S5, Additional File 1). Since tRNAs are not polyadenylated, they were not found in our RNAseq dataset (Materials and Methods). Annotated protein-coding genes lacking RNAseq evidence are mostly orthologs of *Plasmodium falciparum* apicoplast proteins with mid-blood stage expression [24, 25], *T. parva* repeat (*Tpr*) family proteins, or DUF529 domain-containing proteins (Supplementary Table S5, Additional File 1). These

data are consistent with a study published in 2005, which used MPSS to estimate expression levels of *T. parva* genes in the schizont stage of the parasite [26], as well as a more recent study comparing gene expression between the schizont and the sporozoite/sporoblast stages [27]. The expression levels in the sense strand for each gene, as quantified by RPKM, when log-transformed, followed a unimodal distribution similar to a normal distribution (Fig. 3a).

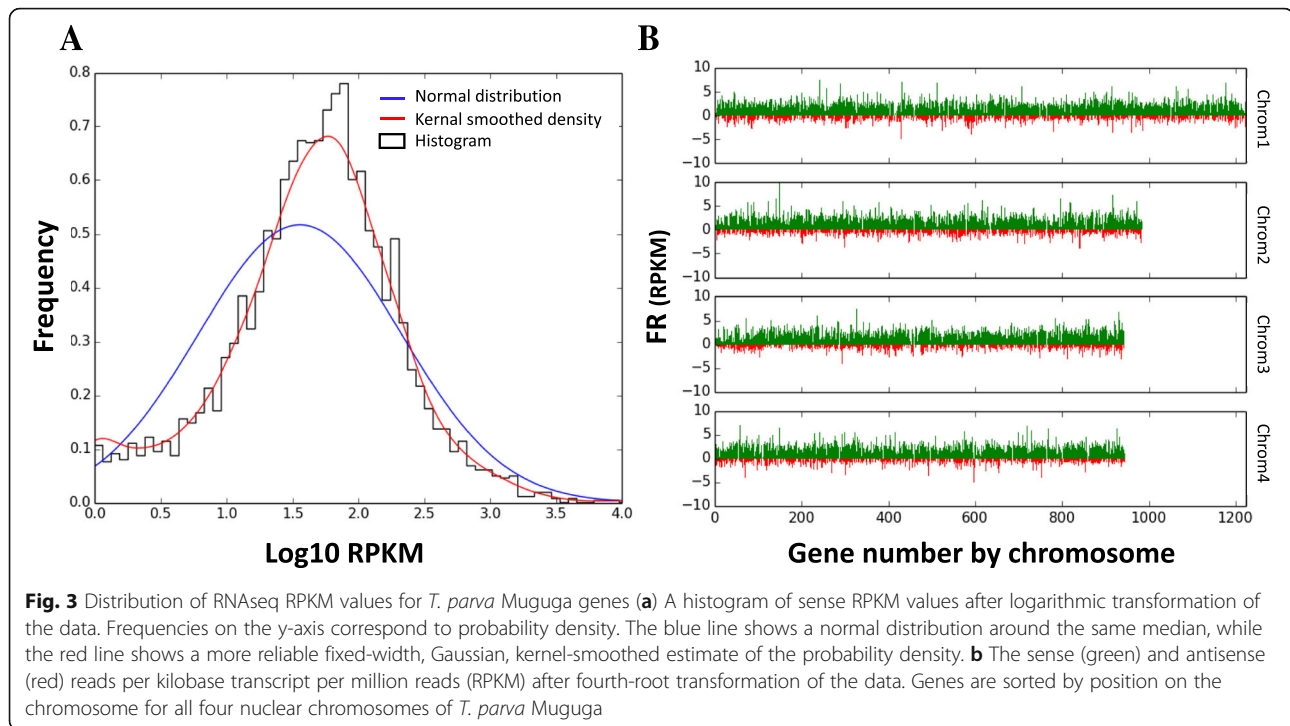
T. parva multi-gene families show variable expression levels

Large gene families are known to play a role in the pathogenesis of protozoan infections, perhaps the most well-known being the *var* gene family in *P. falciparum*. These genes encode proteins that are essential for the sequestration of infected red blood cells, a critical biological feature determining severe malaria pathology of *P. falciparum* [28]. Using the OrthoMCL algorithm as described previously [19], we clustered paralogs in this genome, identifying changes in the size of several of the largest *T. parva* gene families (Supplementary Table S6, Additional File 1), and finding variable patterns in their levels of expression (Supplementary Figure S6, Additional File 1). The roles of most of these gene families are not known. For example, the *Tpr* (*T. parva* repeat) gene family has been suggested to be rapidly evolving and expressed as protein in the piroplasm stages [19]. This is consistent with our findings, which show *Tpr* genes not to be highly expressed in the schizont (Supplementary Figure S6, Additional File 1) or the sporoblast (Supplementary Figure S7, Additional File 1) stages [27, 29]. Interestingly, in that same dataset, we find a significant up-regulation of subtelomeric variable secreted protein gene (SVSP) family genes in the sporozoite stages relative to both the sporoblast and schizont stages, suggesting that they may be important for invasion or the establishment of infection in the vertebrate host (Supplementary Figure S7, Additional File 1) [30].

This new *T. parva* genome annotation not only improved our resolution of the gene models of multi-gene family members and other transformation factors (Supplementary Figure S8, Additional File 1) [31], but also uncovered 128 genes that were not present in the original annotation.

A mechanism of core N-glycosylation is now predicted in *T. parva*

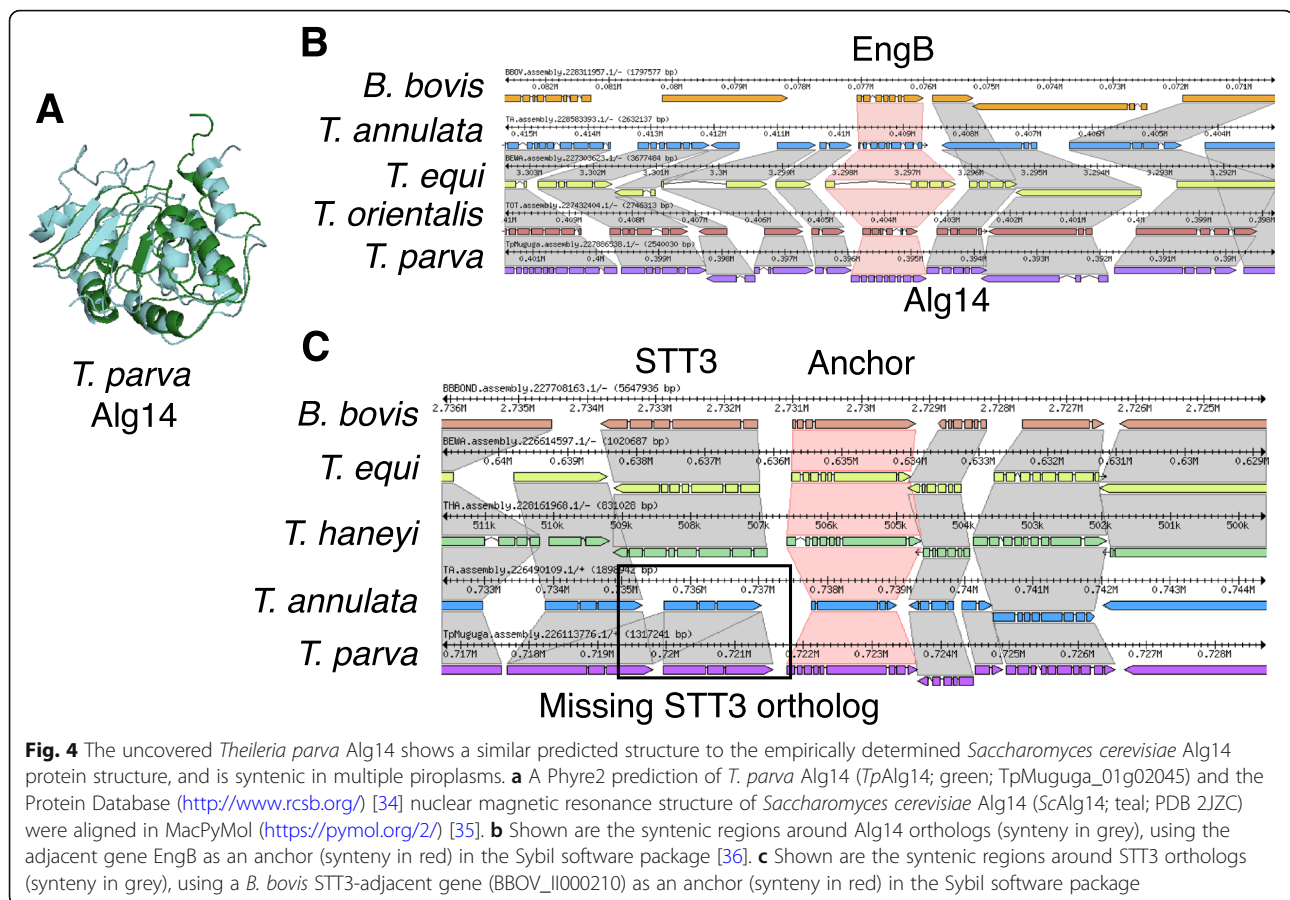
Among the 128 newly identified genes, one was annotated as a potential Alg14 ortholog, an important part of a glycosyltransferase complex in many organisms that add a N-acetylglucosamine (GlcNAc) to the N-glycan precursor. N-glycosylation is an important type of protein post-translational modification, during which a sugar is linked to the nitrogen of specific amino acid residues, a process that occurs in the membrane of the endoplasmic reticulum and is critical for both the structure and



function of many eukaryotic proteins. N-glycosylation is a ubiquitous protein modification process, but the glycans being transferred differ among the domains of life [32]. However, in apicomplexan parasites that infect red blood cells, there appears to be a selection against long N-glycan chains [33]. *Theileria* parasites were previously believed to not add N-acetylglucosamine to their glycan precursors, since sequence similarity searches did not identify the necessary enzymes. While the study by Samuelson and Robbins [33] did not discover any Alg enzymes, we find that *T. parva* has Alg7 (*TpAlg7*; *TpMuguga_01g00118*), Alg13 (*TpAlg13*; *TpMuguga_02g00515*), and Alg14 (*TpAlg14*; *TpMuguga_01g02045*) homologs, which show differential mRNA-level expression between the sporozoite and schizont life cycle stages (Supplementary Figure S9, Additional File 1). In fact, the structure of each of these *Theileria* proteins can be predicted ab initio with high confidence (Supplementary Table S7, Additional File 1) and have predicted secondary structural characteristics very similar to their homologs in *Saccharomyces cerevisiae* (Fig. 4a). However, the structure of the *TpAlg7*-encoding locus was altered as a result of the re-annotation effort and *TpAlg14* is the product of a newly identified gene, which might have prevented the original identification of the pathway. Therefore, *Theileria* parasites likely have a minimal N-glycosylation system. Interestingly, we can find Alg14 orthologs by blastp search in *T. orientalis* (TOT_010000184), *T. equi* (BEWA_032670), but not in *T. annulata*. Using the adjacent gene, EngB, as a marker, a

look at the *T. annulata* genomic region that is syntenic to *TpAlg14* revealed that *T. annulata* has a hypothetical gene annotated on the opposite strand (Fig. 4b), which could be an incorrect annotation. A tblastn search of the *T. annulata* genome using *TpAlg14* led to the discovery of a nucleotide sequence which translated results in an alignment with E-value of 7×10^{-15} and 70% identity over the length of the protein, suggesting the existence of an *T. annulata* Alg14 ortholog (*TaAlg14*). In fact, the gene model that was at the *TpAlg14* locus in the original annotation, TP01_0196, was likely a result of an incorrect annotation transfer from *T. annulata* (or vice-versa), since TP01_0196 shared 52% identity with the gene annotated on the opposite strand at the putative *TaAlg14* locus (E-value 4×10^{-131}). Since previous studies have used *T. annulata* as a model *Theileria* parasite, this could be the reason that N-glycosylation was not discovered in this parasite genus.

While the presence of N-glycans in *Plasmodium* parasite proteins was initially controversial [37], more recent work provided evidence of short N-glycans on the exterior of *P. falciparum* schizonts and trophozoites [38]. As a key difference, *Plasmodium* parasites have a clear ortholog of the oligosaccharyl transferase STT3 (EC 2.4.99.18, PF3D7_1116600 in *P. falciparum* 3D7), which catalyzes the transfer of GlcNAc and GlcNAc₂ to asparagine residues in nascent proteins, and recent work has identified several other proteins in this protein complex in *Plasmodium* genomes [37]. No such ortholog was found in *T. parva* Muguga or *T. annulata* Ankara by



blastp or tblastn searches with the *Plasmodium* protein. Since there are STT3 orthologs in *T. equi* and *T. haneyi* (Fig. 4c), as well as *Cytauxoon felis*, it appears that the absence of STT3 in *T. parva* and *T. annulata* represents evolutionary loss of STT3 orthologs in this lineage. This means that while lipid precursor N-glycosylation does likely occur at the ER in these two species, the canonical mechanism of N-glycan precursor transfer to proteins is apparently absent.

Discussion

The re-annotation of the *T. parva* genome has resulted in significant improvement to the accuracy of gene models, showing that this genome is even more gene-dense than previously thought, with the addition of 2.4% of the genome to CDSs as well as the discovery of additional overlapping genes. This re-annotation has improved our understanding of the biology of the parasite, from contributions of both single copy genes [39] and multi-gene families. Multi-gene families appear to have played a prominent role in the evolution of the lineage leading to *T. parva* and *T. annulata* [40], implying a role for these genes in host-pathogen interactions. These genes have diversified and/or expanded in copy number,

possibly as an adaptation to a particular niche, since the high density of the genome is strongly suggestive of selection against non-functional DNA. We now have a clearer picture of the structure, copy number, and relative expression level of these genes. In addition, a recently generated sporozoite and sporoblast datasets opens up new opportunities to study differential gene expression throughout other stages of the parasite life cycle [27].

The model of transcription that emerges from these recent studies is one of ubiquitous transcription of most genes in the schizont stage, but with a wide range of expression levels [18, 26, 27], suggesting that there are likely important *cis* regulatory motifs that control the level of expression or mRNA stability [18, 41]. Transcription can also arise from potential bidirectional and cryptic promoters with highly prevalent antisense transcription. It remains to be determined if sense and antisense transcripts are generated in the same or different cells in culture, an issue that may be addressed with single-cell RNAseq. Due to the short-read nature of our sequencing platform, we were only able to accurately annotate the most prevalent isoform of each gene. The sequencing of full-length transcripts, for example with Pacific Biosciences sequencing technology, would

provide a more comprehensive description of the *T. parva* transcriptome, including alternatively spliced variants and the boundaries of overlapping transcripts.

In yeast and humans, antisense transcription, defined by the existence of non-coding RNA encoded on the DNA strand opposite to, and overlapping with, that encoding the mRNA, is rare compared to sense transcription [42]. In *T. parva*, however, antisense transcription is highly prevalent throughout the genome (Fig. 3b), as has been found in *P. falciparum*, where antisense transcription is synthesized largely by RNA polymerase II [43, 44] and can alter the expression of multigene family members by regulating the packaging of these loci into chromatin [45]. Most of the antisense transcripts seem to completely overlap with their sense counterparts, although the functional relevance of this observation has yet to be determined.

The discovery of evidence that N-glycosylation may occur in *Theileria* parasites could open up novel treatment options against *Theileria* infections. N-glycosylation is thought to be important for *Toxoplasma gondii* invasion, growth, and motility [46–48]. While the results are somewhat confounded by a lack of inhibitor specificity, treatment with the N-glycosylation inhibitor tunicamycin results in parasites with abnormal endoplasmic reticulum, malformed nuclei, and impaired secretory organelles [49]. While once controversial due to differences in analytical methods, parasite life-cycle stages, and host contamination, *P. falciparum* is now thought to have N-glycosylated proteins, although this is not as frequent a mechanism of protein modification as glycosylphosphatidylinositol [50]. This work has been supported by bioinformatic analyses, finding that *P. falciparum* contains glycosyltransferases (albeit few) [51]. Early work using N-glycosylation inhibitors has shown strong in vitro growth inhibition of *Plasmodium* asexual blood stages [52–56], but the function of N-glycosylation of apicomplexan parasite proteins is a topic that requires further study. Importantly, the lack of an STT3 ortholog in *T. parva*, if true, would suggest that protein-targeted N-glycosylation does not occur in this parasite (as does in *Plasmodium*), and may only occur on the ER and potentially the surface of the parasite. Even though cytoplasmic N-glycosyltransferases have been found in bacteria, they have not been found in eukaryotes, and their presence in *T. parva* seems unlikely. The absence of a N-glycan protein transfer system is largely supported by genome-wide searches for the enrichment of N-glycan acceptor sites in *T. annulata* [57]. While N-glycosylation is often touted as an ‘essential’ protein modification in eukaryotes [58], the absence of an STT3 ortholog in some *Theileria* species suggests that this process may be critical as a lipid, rather than protein, modification. This does not diminish the potential relevance of N-glycosylation in these parasites. Regardless of whether these short N-glycans provoke host immune responses or play a

homeostatic role in parasite protein folding, they could be important therapeutic targets. Finally, given the possibility that glycans encode immunological ‘self’, ‘non-self’ or ‘damage’ identities [59], it is tempting to speculate that the absence of proteinaceous N-glycans in *Theileria* species could represent an evolutionary adaptation to immune evasion in a parasite lineage that resides free in the host cytoplasmic environment.

Conclusions

This study emphasizes the critical interplay between genome annotations and our knowledge of pathogen biology. The significant improvement of the *T. parva* Muguga reference genome gene annotation will facilitate numerous studies of this parasite, and has already given better resolution to genome-wide patterns of gene transcription, including antisense transcription and transcription of multi-gene families. The better the resolution at which we understand gene structure and expression, the more accurately we can characterize and study gene function, novel druggable pathways suitable for interventions and, ultimately, the biology of the pathogen in its different host organisms. For example, the discovery of N-glycosylation precursors in some *Theileria* parasites in the absence of a protein transfer system opens up new questions about the role of lipid N-glycosylation precursors in eukaryote biology as well as the potential evolutionary reasons why protein N-glycosylation would be lost in this apicomplexan lineage.

Methods

RNA sample generation and sequencing

An RNA sample was obtained from a culture of the reference *T. parva* isolate (Muguga), from the haploid schizont stage of the parasite life cycle, which proliferates in host lymphocytes. The extraction method included complement lysis of schizont-infected host lymphocytes, DNase digestion of contaminating host DNA and differential centrifugation to enrich for schizonts [26, 60]. PolyA-enriched RNA was sequenced using Illumina sequencing technology, to produce strand-specific RNAseq data. RNAseq reads were aligned with TopHat and RPKM values calculated using HTseq [61].

Genome re-annotation

For the re-annotation of the *Theileria parva* genome, a number of evidence tracks were generated and loaded into the genome browser JBrowse [62] for manual curation using the WebApollo plugin [63]. RNAseq reads were aligned to the genome with TopHat [64], a splice-aware alignment tool (Supplementary Table S1, Additional File 1). These alignments were used to generate strand-specific read alignment coverage glyphs and XY plots for visualization in WebApollo. TopHat alignment also yields a file of all reported splice junctions using segmented

mapping and coverage information, which is useful for curating intron splice sites. RNAseq reads were also assembled into transcripts using CuffLinks [65] and mapped to the genome with TopHat. We also generated two genome-dependent Trinity/PASA [66] transcriptome assemblies (one reference annotation-dependent and one independent of the reference annotation), as well as one completely de novo Trinity transcriptome assembly. A variety of other proteome data were aligned to the genome with AAT [67] and used as evidence tracks, including previously generated *Theileria annulata* mass spectrometry data [68], and all non-*Theileria* apicomplexan proteins from NCBI's RefSeq.

In order to assess gene prediction accuracy before the manual curation phase, a set of 342 high-confidence *T. parva* gene models were selected from the current reference annotation on the basis of two criteria: (1) RNAseq reads must cover each exon in the gene, (2) Trinity de novo assembled transcripts and read coverage must be concordant with the presence or absence of any introns in the gene model. Out of these 342 genes, 50 were randomly selected as a validation set and the remaining 292 were used as a training gene set for gene prediction software. The exon distribution of the validation set closely resembles that of the training set (Supplementary Table S8, Additional File 1).

Multiple gene prediction software tools were used and then assessed by the accuracy with which they predict the validation set using an in-house script. These included: *i*) Augustus [69], using RNAseq reads, the *T. parva* training gene set, or no evidence; *ii*) Semi-HMM-based Nucleic Acid Parser (SNAP) [70] and Glimmer [71] were trained with the *T. parva* training set; *iii*) Fgenesh [72] used a pre-existing training set of *Plasmodium* genes from its website; *iv*) the ab initio predictor GeneMark-ES [73]. Finally, gene models were selected with the consensus predictor Evidence Modeler (EVM) [74], using 57, differently-weighted combinations of the other evidence, while maximizing prediction accuracy (Supplementary Figure S8, Additional File 1). Based on their performance in comparison with the validation set, only the top four EVM predictions were loaded as evidence tracks for use in manual curation (Supplementary Figure S10, Additional File 1). tRNA and rRNA predictions were generated using tRNAscan-SE [75] and RNAmmer [76] and loaded as evidence tracks, along with the original *T. parva* Muguga annotation (Supplementary Figures S11, S12, Additional File 1). A genome-wide, double-pass, manual curation of all gene models was completed, weighing the RNAseq evidence over the evidence from alignments with homologs from other species and the gene prediction programs. The annotation assignments were allocated in 50 kb segments, with different annotators doing adjacent segments, as well as altering the annotator for

the first and second pass in order to reduce annotator bias.

Functional annotation of the *T. parva* proteome consisted of HMM3 searches of the complete proteome against our custom HMM collection that includes TIGRFams [77], Pfams [78], as well as custom-built HMMs [79] and RAPSearch2 searches against UniRef100 (with a cutoff of 1×10^{-10}). In addition, a TMHMM search which was used to assign “putative integral membrane protein” to proteins with 3 or more helical spans (assuming there were no other hits to the previous searches). These searches were synthesized using Attributor (<https://github.com/jorvis/Attributor>) to generate the final annotation based on the different evidence sources to assign gene product names, EC numbers, GO terms and gene symbols to genes, conservatively where possible.

Multi-gene family clustering

Genes were clustered with OrthoMCL, using an inflation value of 4 and a BLAST *p*-value cutoff of 10^{-5} , as previously done [19]. All individual conserved domain searches were done using NCBI's Conserved Domain Database version 3.11 [80] with 45,746 PSSMs, with an E-value threshold of 0.01 and a composition based statistics adjustment. HMM searches of the entire PFAM database were done using default settings.

Supplementary information

Supplementary information accompanies this paper at <https://doi.org/10.1186/s12864-020-6683-0>.

Additional file 1: Supplemental Figure S1. Architecture of the *Theileria parva* Muguga genome and associated new structural annotation and RNAseq expression data. **Supplemental Figure S2.** Updated gene annotation efforts in the *Theileria parva* genome reveal the existence of many genes that overlap adjacent genes at either UTR or CDS sequences. **Supplemental Figure S3.** RNA-seq reads that map to introns in the *Theileria parva* Muguga genome support the existence of genes where a subset of introns are not spliced. **Supplemental Figure S4.** Histogram of mRNA length across all annotated transcripts in the current *T. parva* Muguga annotation. **Supplemental Figure S5.** Types of transcription initiated in *Theileria parva*. **Supplemental Figure S7.** The expression distribution of three selected gene families in *T. parva* Muguga (SVSP = subtelomeric variable secreted protein gene family; Tpr = *T. parva* repeat gene family; TashAT = *Theileria annulata* schizont AT hook gene family). **Supplemental Figure S8.** *Theileria* PIN1 is an example of a parasite-secreted protein that plays a role in host transformation. **Supplemental Figure S9.** The expression N-glycosylation pathway components in the sporozoite and schizont life cycle stages of *T. parva* Muguga. **Supplemental Figure S10.** A representation of the relative weights of each evidence in each EVM prediction tested. **Supplemental Figure S11.** The percentage of validated genes, or coding exons correctly predicted by EVM with each evidence combination. **Supplemental Figure S12.** A comparison of the prediction accuracy of each gene predictor used in this study. **Supplemental Table S1.** RNAseq read counts, length and GC content of each *T. parva* chromosome. **Supplemental Table S2.** A comparison of genome characteristics of *T. parva* Muguga to several other piroplasms and *Plasmodium falciparum* 3D7. **Supplemental Table S3.** A list of the expression levels (RPKM = reads per kilobase of transcript per million reads) of known *T. parva* antigens. **Supplemental Table S4.** A list of the most highly-expressed genes in the *T. parva* schizont RNAseq

dataset. **Supplemental Table S5.** A table of key *T. parva* genes with reads per kilobase of transcript per million reads of zero. (Tp = Theileria parva Muguga; Pf = *Plasmodium falciparum* 3D7). **Supplemental Table S6.** A description of the top 20 largest multi-gene families defined by OrthoMCL in *T. parva* Muguga and their conservation in *T. annulata* (Ta), *T. orientalis* (To), and *T. equi* (Te), as defined by Jaccard-filtered clusters of orthologous genes. **Supplemental Table S7.** Summary of the top-ranked Phyre2 hits for each proposed Alg homolog discussed in this study. **Supplemental Table S8.** The exon distribution of the validation and training sets used for gene prediction.

Additional file 2. Pairs of consecutive genes with overlap in UTR only or both UTR and CDS.

Additional file 3. Ratio of intron_coverage by average_CDS_coverage, for introns with read_coverage > 0.

Abbreviations

ECF: East coast fever; UTR: Untranslated regions; CDS: Coding sequence; RPKM: Reads per kilobase of transcript, per million mapped reads; Tpr: *T. parva* repeat family; SVSP: Subtelomeric variable secreted protein; SNAP: Semi-HMM-based nucleic acid parser

Acknowledgements

We would like to thank Donald P. Knowles for his kind and helpful feedback and support for this project.

Authors' contributions

JCS, RP, RPB, CD, VMN, and LF conceived the study design. RP isolated *T. parva* schizont RNA for RNAseq using differential centrifugation and standard kits as described. JO, OOI, and PK built and maintained the JBrowse instance, used for manual curation using the WebApollo plugin, as well as the functional annotation pipeline, used to attribute product names. They also generated in-house scripts as necessary for analysis. KT, JO, HTG, OOI, PK, and SBAL generated alignment tracks to assist the annotation. KT, HTG, OOI, NCP, SBAL, JCS completed manual re-annotation of the genome. KT performed all other analyses. KT and JCS wrote the manuscript. All authors critically reviewed and approved the manuscript.

Funding

This work was supported in part by the by the Bill and Melinda Gates Foundation (OPP1078791, to JCS) and by the United States Department of Agriculture, Agricultural Research Service (USDA-ARS; through agreement #59-5348-4-001 to JCS), both of which contributed to personnel (HTG, OOI, PK, NCP, SBAL, JCS), sequencing and analysis support. Immunity and Infection T32 training grant NIH/NIAID T32 AI007540-14 provided stipend support (KT).

Availability of data and materials

The *T. parva* Muguga re-annotation can be visualized at the following online link (http://jbrowse.igs.umaryland.edu/t_parva/), and can be downloaded from NCBI's BioProject database, with project number PRJNA16138. The schizont-stage RNAseq data has Short Read Archive (SRA) accession number SRR3001169.

Ethics approval and consent to participate

This study was carried out in strict accordance with the recommendations in the standard operating procedures of the Institutional Animal Care and Use Committee (IACUC) of the International Livestock Research Institute (ILRI), in Nairobi, Kenya. ILRI's IACUC was established in 1993, and the institute complies voluntarily with the UK's Animals (Scientific Procedures) Act 1986 (<http://www.homeoffice.gov.uk/science-research/animal-research/>) that contains guidelines and codes of practice for the housing and care of animals used in scientific procedures. Schizont-infected lymphocyte cultures were derived from lymph node biopsies taken from cattle experimentally infected with *T. parva* sporozoite stabilates, as described in Morzaria et al. [81]. The studies in which cattle were infected were specifically approved by ILRI's IACUC. The expansion of the infected lymphocyte cultures, conducted to generate the material used in this study, does not necessitate explicit IACUC approval.

Consent for publication

Not applicable.

Competing interests

The authors declare that they have no competing interests.

Author details

¹Institute for Genome Sciences, University of Maryland School of Medicine, Baltimore, MD 21201, USA. ²Biosciences Eastern and Central Africa, International Livestock Research Institute, Nairobi, Kenya. ³Animal Disease Research Unit, Agricultural Research Service, USDA, Pullman, WA 99164, USA. ⁴Department of Veterinary Microbiology & Pathology, Washington State University, Pullman, WA 99164, USA. ⁵International Livestock Research Institute, Nairobi, Kenya. ⁶Swiss Tropical and Public Health Institute, Basel, Switzerland. ⁷University of Basel, Basel, Switzerland. ⁸Department of Microbiology and Immunology, University of Maryland School of Medicine, Baltimore, MD 21201, USA.

Received: 27 August 2019 Accepted: 18 March 2020

Published online: 03 April 2020

References

1. Spielman DJ. XVI public-private partnerships and pro-poor livestock research: the search for an East Coast fever vaccine, vol. 1. Washington, D.C.: The National Academies Press; 2009.
2. Herrero M, Thornton PK, Notenbaert AM, Wood S, Msangi S, Freeman HA, Bossio D, Dixon J, Peters M, van de Steeg J, et al. Smart investments in sustainable food production: revisiting mixed crop-livestock systems. *Science*. 2010;327(5967):822–5.
3. Nkedianye D, Radeny M, Kristjanson P, Herrero M. Assessing returns to land and changing livelihood strategies in Kitengela. In: Homewood K, Kristjanson P, Chevenix Trench P, editors. *Staying Maasai? Livelihoods, conservation and development in East African Rangelands*. Dordrecht: Springer; 2009. p. 115–50.
4. Baldwin CL, Black SJ, Brown WC, Conrad PA, Goddeeris BM, Kinuthia SW, Lalor PA, MacHugh ND, Morrison WJ, Morzaria SP, et al. Bovine T cells, B cells, and null cells are transformed by the protozoan parasite *Theileria parva*. *Infect Immun*. 1988;56(2):462–7.
5. Tindih HS, Geysen D, Goddeeris BM, Awino E, Dobbelaere DA, Naessens J. A *Theileria parva* isolate of low virulence infects a subpopulation of lymphocytes. *Infect Immun*. 2012;80(3):1267–73.
6. Irvin AD, Mwamachi DM. Clinical and diagnostic features of East Coast fever (*Theileria parva*) infection of cattle. *Veterinary Record*. 1983;113(9):192–8.
7. Fry LM, Schneider DA, Frevert CW, Nelson DD, Morrison WJ, Knowles DP. East Coast fever caused by *Theileria parva* is characterized by macrophage activation associated with Vasculitis and respiratory failure. *PLoS One*. 2016; 11(5):e0156004.
8. Hotez PJ, Molyneux DH, Fenwick A, Kumaresan J, Sachs SE, Sachs JD, Savioli L. Control of neglected tropical diseases. *N Engl J Med*. 2007;357(10):1018–27.
9. Reed SL, McKerrow JH. Why funding for neglected tropical diseases should be a global priority. *Clin Infect Dis*. 2018;67(3):323–6.
10. Sette A, Rappuoli R. Reverse vaccinology: developing vaccines in the era of genomics. *Immunity*. 2010;33(4):530–41.
11. Seib KL, Dougan G, Rappuoli R. The key role of genomics in modern vaccine and drug design for emerging infectious diseases. *PLoS Genet*. 2009;5(10):e1000612.
12. Hotez PJ, Fenwick A, Ray SE, Hay SI, Molyneux DH. "Rapid impact" 10 years after: the first "decade" (2006-2016) of integrated neglected tropical disease control. *PLoS Negl Trop Dis*. 2018;12(5):e0006137.
13. Chaudhary K, Roos DS. Protozoan genomics for drug discovery. *Nat Biotechnol*. 2005;23(9):1089–91.
14. Oberg AL, Kennedy RB, Li P, Ovsyannikova IG, Poland GA. Systems biology approaches to new vaccine development. *Curr Opin Immunol*. 2011;23(3):436–43.
15. Wakaguri H, Suzuki Y, Sasaki M, Sugano S, Watanabe J. Inconsistencies of genome annotations in apicomplexan parasites revealed by 5'-end-one-pass and full-length sequences of oligo-capped cDNAs. *BMC Genomics*. 2009;10:312.
16. Yeoh LM, Lee W, McFadden GI, Ralph SA. Alternative Splicing in Apicomplexan Parasites. *MBio*. 2019;10(1):e02866–18.
17. Yandell M, Ence D. A beginner's guide to eukaryotic genome annotation. *Nat Rev Genet*. 2012;13(5):329–42.

18. Tretina K, Pelle R, Silva JC. Cis regulatory motifs and antisense transcriptional control in the apicomplexan *Theileria parva*. *BMC Genomics*. 2016;17(1):128.
19. Gardner MJ, Bishop R, Shah T, de Villiers EP, Carlton JM, Hall N, Ren Q, Paulsen IT, Pain A, Berriman M, et al. Genome sequence of *Theileria parva*, a bovine pathogen that transforms lymphocytes. *Science*. 2005;309(5731):134–7.
20. Pain A, Renaud H, Berriman M, Murphy L, Yeats CA, Weir W, Kerhoun A, Aslett M, Bishop R, Bouchier C, et al. Genome of the host-cell transforming parasite *Theileria annulata* compared with *T. parva*. *Science*. 2005;309(5731):131–3.
21. Collins L, Penny D. Complex spliceosomal organization ancestral to extant eukaryotes. *Mol Biol Evol*. 2005;22(4):1053–66.
22. Russell K, Hasenkamp S, Emes R, Horrocks P. Analysis of the spatial and temporal arrangement of transcripts over intergenic regions in the human malarial parasite *Plasmodium falciparum*. *BMC Genomics*. 2013;14:267.
23. Unlu AH, Tajeri S, Bilgic HB, Eren H, Karagenc T, Langsley G. The secreted *Theileria annulata* Ta9 protein contributes to activation of the AP-1 transcription factor. *PLoS One*. 2018;13(5):e0196875.
24. Painter HJ, Carrasquilla M, Llinas M. Capturing in vivo RNA transcriptional dynamics from the malaria parasite *Plasmodium falciparum*. *Genome Res*. 2017;27(6):1074–1086.
25. Rovira-Graells N, Gupta AP, Planet E, Crowley VM, Mok S, Ribas de Pouplana L, Preiser PR, Bozdech Z, Cortes A. Transcriptional variation in the malaria parasite *Plasmodium falciparum*. *Genome Res*. 2012;22(5):925–38.
26. Bishop R, Shah T, Pelle R, Hoyle D, Pearson T, Haines L, Brass A, Hulme H, Graham SP, Taracha EL, et al. Analysis of the transcriptome of the protozoan *Theileria parva* using MPSS reveals that the majority of genes are transcriptionally active in the schizont stage. *Nucleic Acids Res*. 2005;33(17):5503–11.
27. Tonui T, Corredor-Moreno P, Kanduma E, Njuguna J, Njahira MN, Nyanjom SG, Silva JC, Djikeng A, Pelle R. Transcriptomics reveal potential vaccine antigens and a drastic increase of upregulated genes during *Theileria parva* development from arthropod to bovine infective stages. *PLoS One*. 2018;13(10):e0204047.
28. Deitsch KW, Dzikowski R. Variant gene expression and antigenic variation by malaria parasites. *Annu Rev Microbiol*. 2017;71:625–41.
29. Bishop R, Musoke A, Morzaria S, Sohanpal B, Gobright E. Concerted evolution at a multicopy locus in the protozoan parasite *Theileria parva*: extreme divergence of potential protein-coding sequences. *Mol Cell Biol*. 1997;17(3):1666–73.
30. Schmuckli-Maurer J, Casanova C, Schmiel S, Affentranger S, Parvanova I, Kang'a S, Nene V, Katzer F, McKeever D, Muller J, et al. Expression analysis of the *Theileria parva* subtelomere-encoded variable secreted protein gene family. *PLoS One*. 2009;4(3):e4839.
31. Marsolier J, Perichon M, DeBarry JD, Villoutreix BO, Chluba J, Lopez T, Garrido C, Zhou XZ, Lu KP, Fritsch L, et al. Theileria parasites secrete a prolyl isomerase to maintain host leukocyte transformation. *Nature*. 2015;520(7520):378–82.
32. Schwarz F, Aebi M. Mechanisms and principles of N-linked protein glycosylation. *Curr Opin Struct Biol*. 2011;21(5):576–82.
33. Samuelson J, Robbins PW. Effects of N-glycan precursor length diversity on quality control of protein folding and on protein glycosylation. *Semin Cell Dev Biol*. 2015;41:121–8.
34. Berman HM, Westbrook J, Feng Z, Gilliland G, Bhat TN, Weissig H, Shindyalov IN, Bourne PE. The Protein Data Bank. *Nucleic Acids Res*. 2000;28(1):235–42.
35. Janson G, Zhang C, Prado MG, Paiardini A. PyMod 2.0: improvements in protein sequence-structure analysis and homology modeling within PyMOL. *Bioinformatics*. 2017;33(3):444–6.
36. Riley DR, Angiuoli SV, Crabtree J, Dunning Hotopp JC, Tettelin H. Using Sybil for interactive comparative genomics of microbes on the web. *Bioinformatics*. 2012;28(2):160–6.
37. Tamana S, Promponas VJ. An updated view of the oligosaccharyltransferase complex in *Plasmodium*. *Glycobiology*. 2019;29(5):385–96.
38. Bushkin GG, Ratner DM, Cui J, Banerjee S, Duraisingh MT, Jennings CV, Dvorin JD, Gubbels MJ, Robertson SD, Steffen M, et al. Suggestive evidence for Darwinian selection against asparagine-linked glycans of *Plasmodium falciparum* and *Toxoplasma gondii*. *Eukaryot Cell*. 2010;9(2):228–41.
39. Tretina K, Haidar M, Madsen-Bouterse SA, Sakura T, Mfarrej S, Fry L, Chaussepied M, Pain A, Knowles DP, Nene VM, et al. *Theileria* parasites subvert E2F signaling to stimulate leukocyte proliferation. *Sci Rep*. 2020;10(1):3982.
40. Reid AJ. Large, rapidly evolving gene families are at the forefront of host-parasite interactions in Apicomplexa. *Parasitology*. 2015;142(Suppl 1):S57–70.
41. Pieszko M, Weir W, Goodhead I, Kinnaird J, Shiels B. ApiAP2 factors as candidate regulators of stochastic commitment to Merozoite production in *Theileria annulata*. *PLoS Negl Trop Dis*. 2015;9(8):e0003933.
42. Ozsolak F, Kapranov P, Foissac S, Kim SW, Fishilevich E, Monaghan AP, John B, Milos PM. Comprehensive polyadenylation site maps in yeast and human reveal pervasive alternative polyadenylation. *Cell*. 2010;143(6):1018–29.
43. Miliello KT, Patel V, Chessler AD, Fisher JK, Kasper JM, Gunasekera A, Wirth DF. RNA polymerase II synthesizes antisense RNA in *Plasmodium falciparum*. *RNA*. 2005;11(4):365–70.
44. Lopez-Barragan MJ, Lemieux J, Quinones M, Williamson KC, Molina-Cruz A, Cui K, Barillas-Mury C, Zhao K, Su XZ. Directional gene expression and antisense transcripts in sexual and asexual stages of *Plasmodium falciparum*. *BMC Genomics*. 2011;12:587.
45. Jing Q, Cao L, Zhang L, Cheng X, Gilbert N, Dai X, Sun M, Liang S, Jiang L. *Plasmodium falciparum* var gene is activated by its antisense long noncoding RNA. *Front Microbiol*. 2018;9:3117.
46. Fauqueney S, Morelle W, Hovasse A, Bednarczyk A, Slomianny C, Schaeffer C, Van Dorsselaer A, Tomavo S. Proteomics and glycomics analyses of N-glycosylated structures involved in *Toxoplasma gondii*-host cell interactions. *Mol Cell Proteomics*. 2008;7(5):891–910.
47. Gas-Pascual E, Ichikawa HT, Sheikh MO, Serji MI, Deng B, Mandalasi M, Bandini G, Samuelson J, Wells L, West CM. CRISPR/Cas9 and glycomics tools for *Toxoplasma* glycobiology. *J Biol Chem*. 2019;294(4):1104–25.
48. Sidik SM, Huet D, Ganesan SM, Huynh MH, Wang T, Nasamu AS, Thiru P, Saeji JPJ, Caruthers VB, Niles JC, et al. A genome-wide CRISPR screen in *Toxoplasma* identifies essential Apicomplexan genes. *Cell*. 2016;166(6):1423–35 e1412.
49. Luk FC, Johnson TM, Beckers CJ. N-linked glycosylation of proteins in the protozoan parasite *Toxoplasma gondii*. *Mol Biochem Parasitol*. 2008;157(2):169–78.
50. Cova M, Rodrigues JA, Smith TK, Izquierdo L. Sugar activation and glycosylation in *Plasmodium*. *Malar J*. 2015;14:427.
51. Samuelson J, Banerjee S, Magnelli P, Cui J, Kelleher DJ, Gilmore R, Robbins PW. The diversity of dolichol-linked precursors to Asn-linked glycans likely results from secondary loss of sets of glycosyltransferases. *Proc Natl Acad Sci U S A*. 2005;102(5):1548–53.
52. Trigg PI, Hirst SI, Shakespeare PG, Tappenden L. Labelling of membrane glycoprotein in erythrocytes infected with *Plasmodium knowlesi*. *Bull World Health Organ*. 1977;55(2–3):205–9.
53. Udeinya JJ, Van Dyke K. Labelling of membrane glycoproteins of cultivated *Plasmodium falciparum*. *Bull World Health Organ*. 1980;58(3):445–8.
54. Udeinya JJ, Van Dyke K. *Plasmodium falciparum*: synthesis of glycoprotein by cultured erythrocytic stages. *Exp Parasitol*. 1981;52(3):297–302.
55. Udeinya JJ, Van Dyke K. Concurrent inhibition by tunicamycin of glycosylation and parasitemia in malarial parasites (*Plasmodium falciparum*) cultured in human erythrocytes. *Pharmacology*. 1981;23(3):165–70.
56. Udeinya JJ, Van Dyke K. 2-Deoxyglucose: inhibition of parasitemia and of glucosamine incorporation into glycosylated macromolecules, in malarial parasites (*Plasmodium falciparum*). *Pharmacology*. 1981;23(3):171–5.
57. Cui J, Smith T, Robbins PW, Samuelson J. Darwinian selection for sites of Asn-linked glycosylation in phylogenetically disparate eukaryotes and viruses. *Proc Natl Acad Sci U S A*. 2009;106(32):13421–6.
58. Lombard J. The multiple evolutionary origins of the eukaryotic N-glycosylation pathway. *Biol Direct*. 2016;11:36.
59. Mavarakis E, Kim K, Shimoda M, Gershwin ME, Patel F, Wilken R, Raychaudhuri S, Ruhaak LR, Lebrilla CB. Glycans in the immune system and the altered glycan theory of autoimmunity: a critical review. *J Autoimmun*. 2015;57:1–13.
60. Graham SP, Pelle R, Honda Y, Mwangi DM, Tonukari NJ, Yamage M, Glew EJ, de Villiers EP, Shah T, Bishop R, et al. *Theileria parva* candidate vaccine antigens recognized by immune bovine cytotoxic T lymphocytes. *Proc Natl Acad Sci U S A*. 2006;103(9):3286–91.
61. Anders S, Pyl PT, Huber W. HTSeq—a Python framework to work with high-throughput sequencing data. *Bioinformatics*. 2015;31(2):166–9.
62. Skinner ME, Uzilov AV, Stein LD, Mungall CJ, Holmes IH. JBrowse: a next-generation genome browser. *Genome Res*. 2009;19(9):1630–8.
63. Lee E, Helt GA, Reese JT, Munoz-Torres MC, Childers CP, Buels RM, Stein L, Holmes IH, Elisk CG, Lewis SE. Web Apollo: a web-based genomic annotation editing platform. *Genome Biol*. 2013;14(8):R93.
64. Kim D, Perte G, Trapnell C, Pimentel H, Kelley R, Salzberg SL. TopHat2: accurate alignment of transcriptomes in the presence of insertions, deletions and gene fusions. *Genome Biol*. 2013;14(4):R36.
65. Roberts A, Pimentel H, Trapnell C, Pachter L. Identification of novel transcripts in annotated genomes using RNA-Seq. *Bioinformatics*. 2011;27(17):2325–9.
66. Grabherr MG, Haas BJ, Yassour M, Levin JZ, Thompson DA, Amit I, Adiconis X, Fan L, Raychowdhury R, Zeng Q, et al. Full-length transcriptome assembly from RNA-Seq data without a reference genome. *Nat Biotechnol*. 2011;29(7):644–52.

67. Huang X, Adams MD, Zhou H, Kerlavage AR. A tool for analyzing and annotating genomic sequences. *Genomics*. 1997;46(1):37–45.
68. Witschi M, Xia D, Sanderson S, Baumgartner M, Wastling JM, Dobbelaere DA. Proteomic analysis of the *Theileria annulata* schizont. *Int J Parasitol*. 2013;43(2):173–80.
69. Stanke M, Morgenstern B. AUGUSTUS: a web server for gene prediction in eukaryotes that allows user-defined constraints. *Nucleic Acids Res*. 2005; 33(Web Server issue):W465–7.
70. Korf I. Gene finding in novel genomes. *BMC bioinformatics*. 2004;5:59.
71. Delcher AL, Bratke KA, Powers EC, Salzberg SL. Identifying bacterial genes and endosymbiont DNA with glimmer. *Bioinformatics*. 2007;23(6):673–9.
72. Solovyev V, Kosarev P, Seledsov I, Vorobyev D. Automatic annotation of eukaryotic genes, pseudogenes and promoters. *Genome Biol*. 2006;7(Suppl 1):S10 11–12.
73. Borodovsky M, Lomsadze A. Eukaryotic gene prediction using GeneMarkhm-E and GeneMark-ES. *Curr Protoc Bioinformatics*. 2011;Chapter 4(Unit 4 6):1–10.
74. Haas BJ, Salzberg SL, Zhu W, Pertea M, Allen JE, Orvis J, White O, Buell CR, Wortman JR. Automated eukaryotic gene structure annotation using EvidenceModeler and the program to assemble spliced alignments. *Genome Biol*. 2008;9(1):R7.
75. Lowe TM, Eddy SR. tRNAscan-SE: a program for improved detection of transfer RNA genes in genomic sequence. *Nucleic Acids Res*. 1997;25(5):955–64.
76. Lagesen K, Hallin P, Rodland EA, Staerfeldt HH, Rognes T, Ussery DW. RNAMmer: consistent and rapid annotation of ribosomal RNA genes. *Nucleic Acids Res*. 2007;35(9):3100–8.
77. Haft DH, Selengut JD, White O. The TIGRFAMs database of protein families. *Nucleic Acids Res*. 2003;31(1):371–3.
78. Finn RD, Bateman A, Clements J, Coggill P, Eberhardt RY, Eddy SR, Heger A, Hetherington K, Holm L, Mistry J, et al. Pfam: the protein families database. *Nucleic Acids Res*. 2014;42(Database issue):D222–30.
79. Li L, Stoeckert CJ Jr, Roos DS. OrthoMCL: identification of ortholog groups for eukaryotic genomes. *Genome Res*. 2003;13(9):2178–89.
80. Marchler-Bauer A, Bo Y, Han L, He J, Lanczycki CJ, Lu S, Chitsaz F, Derbyshire MK, Geer RC, Gonzales NR, et al. CDD/SPARCLE: functional classification of proteins via subfamily domain architectures. *Nucleic Acids Res*. 2017;45(D1):D200–3.
81. Morzaria SP, Dolan TT, Norval RA, Bishop RP, Spooner PR. Generation and characterization of cloned *Theileria parva* parasites. *Parasitology*. 1995;111(Pt 1):39–49.

Publisher's Note

Springer Nature remains neutral with regard to jurisdictional claims in published maps and institutional affiliations.

Ready to submit your research? Choose BMC and benefit from:

- fast, convenient online submission
- thorough peer review by experienced researchers in your field
- rapid publication on acceptance
- support for research data, including large and complex data types
- gold Open Access which fosters wider collaboration and increased citations
- maximum visibility for your research: over 100M website views per year

At BMC, research is always in progress.

Learn more biomedcentral.com/submissions

